SUPPLEMENTARY INFORMATION

Cryo-EM of human rhinovirus reveals capsid-RNA duplex interactions that provide insights into virus assembly and genome uncoating

David Gil-Cantero[a], Carlos P. Mata[b,1], Luis Valiente[c], Alicia Rodríguez-Huete[c], Alejandro Valbuena[c], Reidun Twarock[d], Peter G. Stockley[b], Mauricio G. Mateu[c,2] and José R. Castón[a,e,2]

[a]Department of Structure of Macromolecules, Centro Nacional de Biotecnología (CNB-CSIC), Campus de Cantoblanco, Madrid, Spain; [b]Astbury Centre for Structural Molecular Biology, Faculty of Biological Sciences, University of Leeds, LS29JT, Leeds, United Kingdom; [c]Centro de Biología Molecular "Severo Ochoa" (CSIC-UAM), Universidad Autónoma de Madrid, Madrid, Spain; [d]Department of Mathematics and Department of Biology, University of York, York, YO10 5DD, United Kingdom; [e]Nanobiotechnology Associated Unit CNB-CSIC-IMDEA, Campus Cantoblanco, Madrid, Spain

[1] Present address: Biocomputing Unit, Department of Structure of Macromolecules, Centro Nacional de Biotecnología (CNB-CSIC), Campus de Cantoblanco, Madrid, Spain

[2]To whom correspondence should be addressed: E-mails: mgarcia@cbm.csic.es, jrcaston@cnb.csic.es

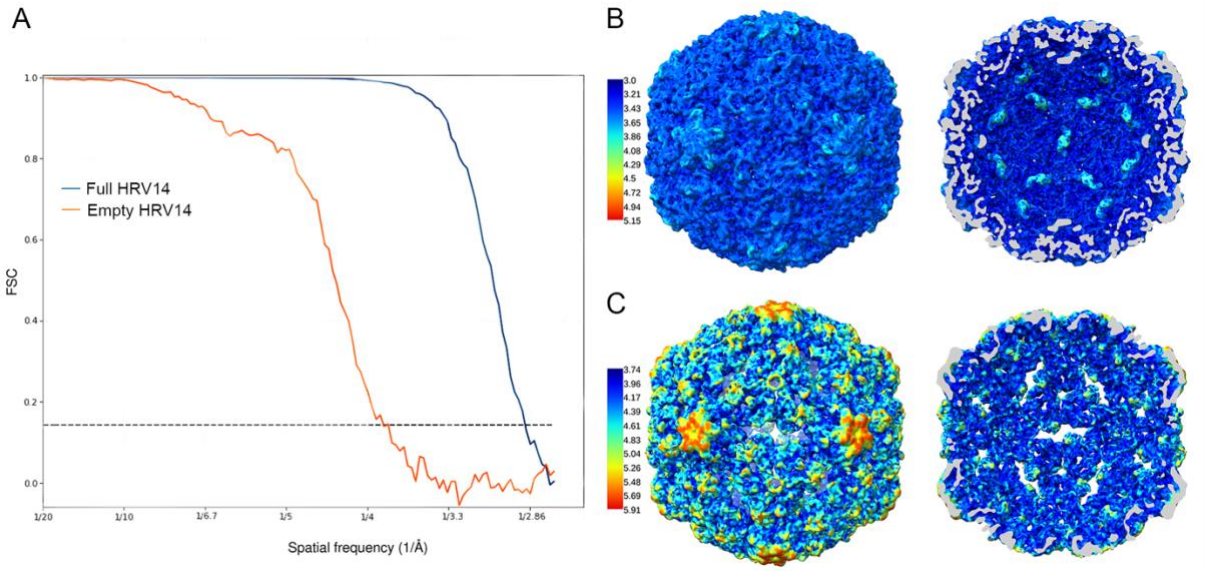

Supplementary Fig. 1. Global and local resolution of cryo-EM maps of full and empty RV-B14 maps. (A) Fourier shell correlation (FSC) curves for full and empty RV-B14. Resolution based on the 0.143 criteria is indicated. For the 0.143 threshold, the values for full and empty RV-B14 were 2.9 and 3.8 Å, respectively. (B, C) Local resolution assessment for full (B) and empty (C) RV-B14 maps. Surface-shaded representations of the RV-B14 capsid outer (left) and inner (right) surfaces viewed along an icosahedral 2-fold axis. The bar indicates the resolution in Å.

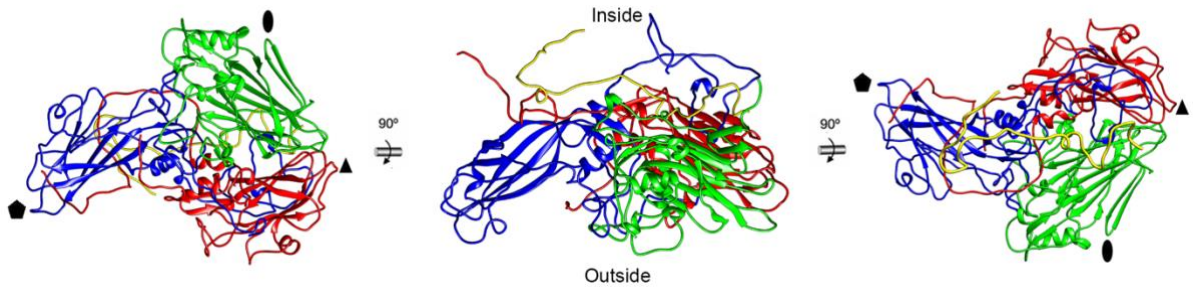

Supplementary Fig. 2. Atomic model of the asymmetric unit (biological protomer) in the RV-B14 virion structure. Ribbon diagrams for VP1 (blue), VP2 (green), VP3 (red) and VP4 (yellow) are represented (top view, left; side view, center; bottom view, right). Black symbols indicate icosahedral symmetry axes.

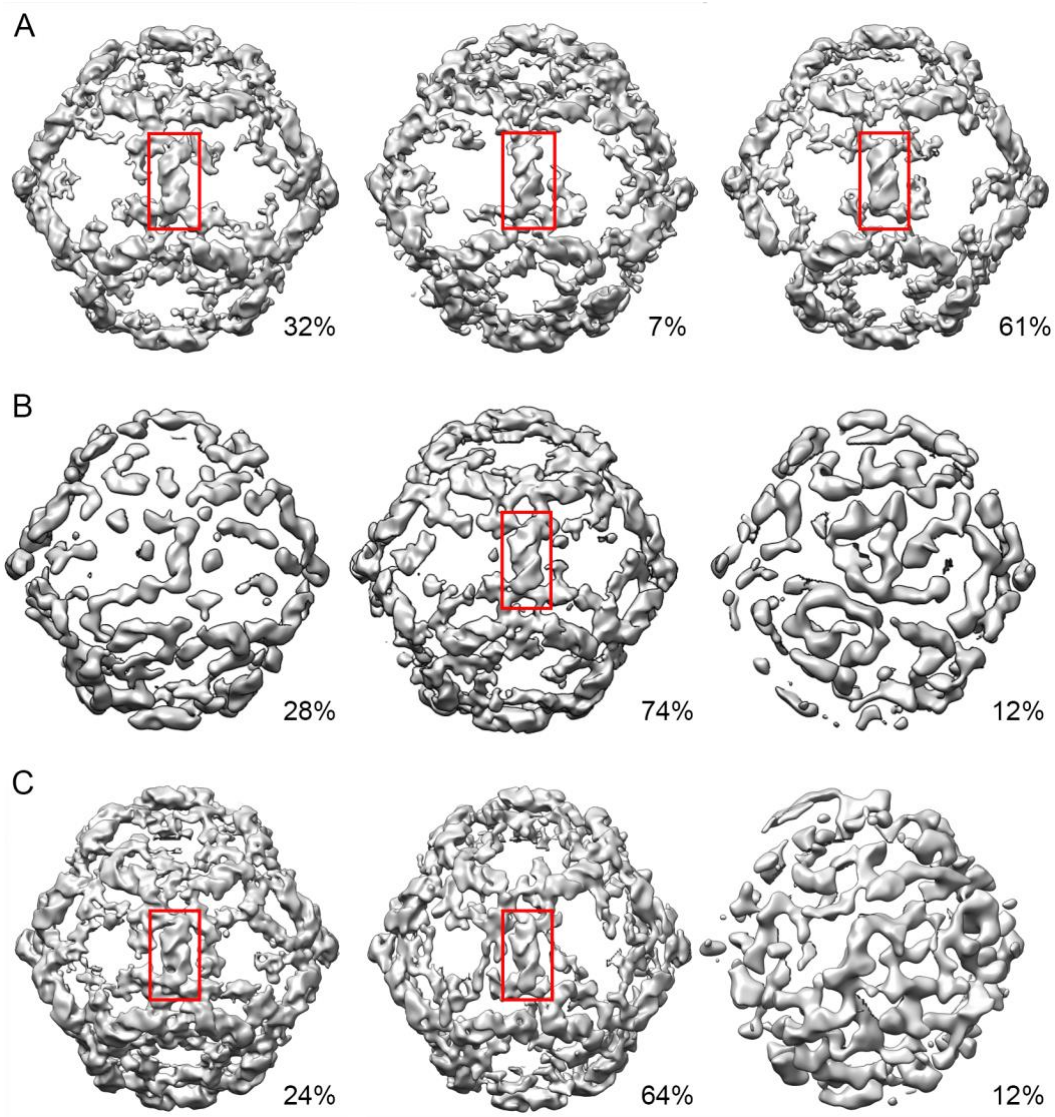

Supplementary Fig. 3. Asymmetric reconstructions for the RV-B14 genome. (A) 3D classification of RV-B14 virions using as initial model an icosahedral map with the genome removed computationally. (B) 3D classification of virion images with the icosahedral capsid removed computationally and using as initial model the genome map obtained in (A) 61%. (C) 3D classification of virion images with the icosahedral capsid removed computationally using as initial model only the genome map obtained after icosahedral refinement.

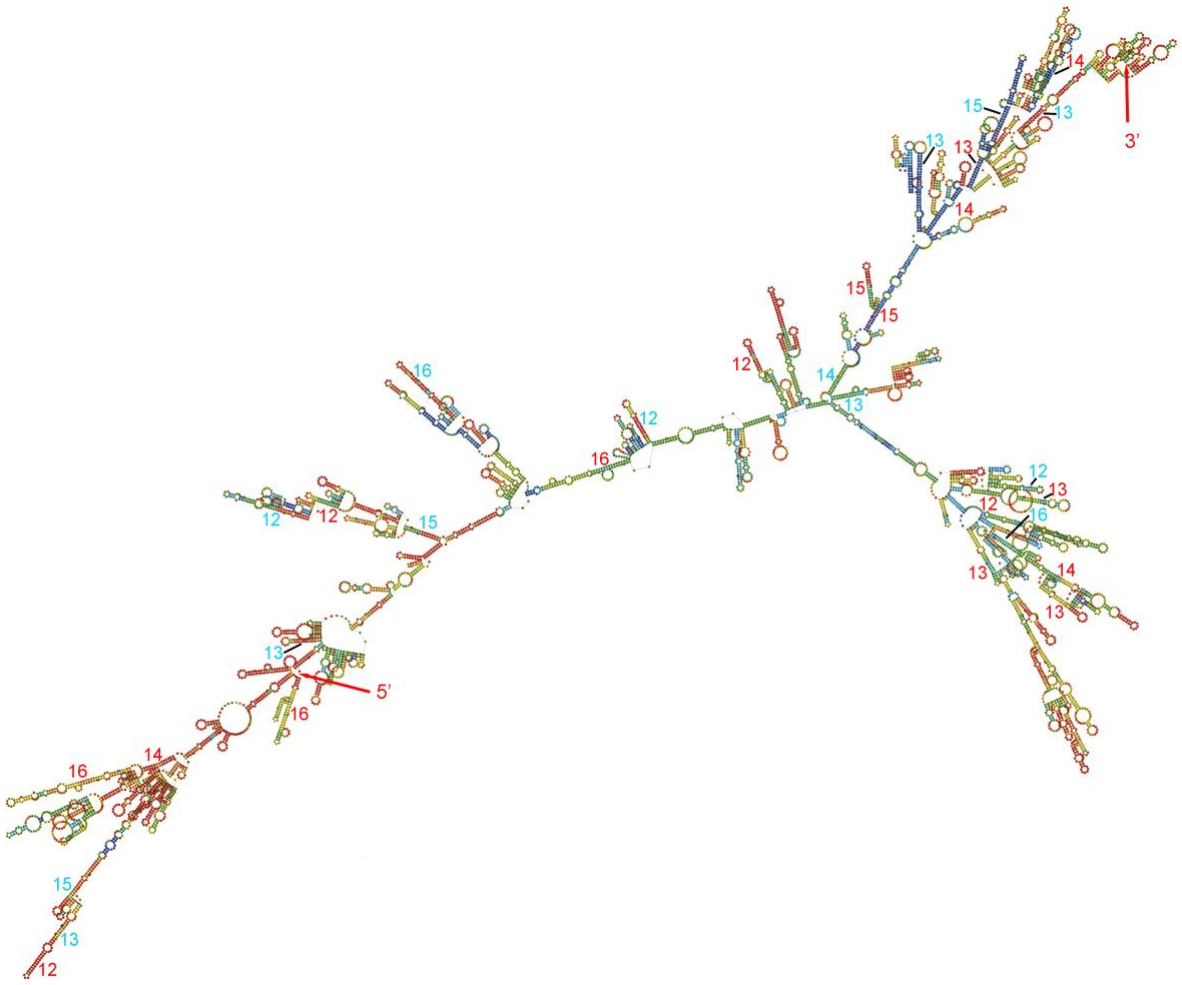

Supplementary Fig. 4. Secondary structure prediction for the ssRNA genome of RV-B14. There are 31 duplexes of 12-16 bp that are candidates for the genome densities located at the two-fold axes (length is indicated; in red and blue, with and without pendant purines, respectively). 5' and 3' ends are indicated with red arrows.

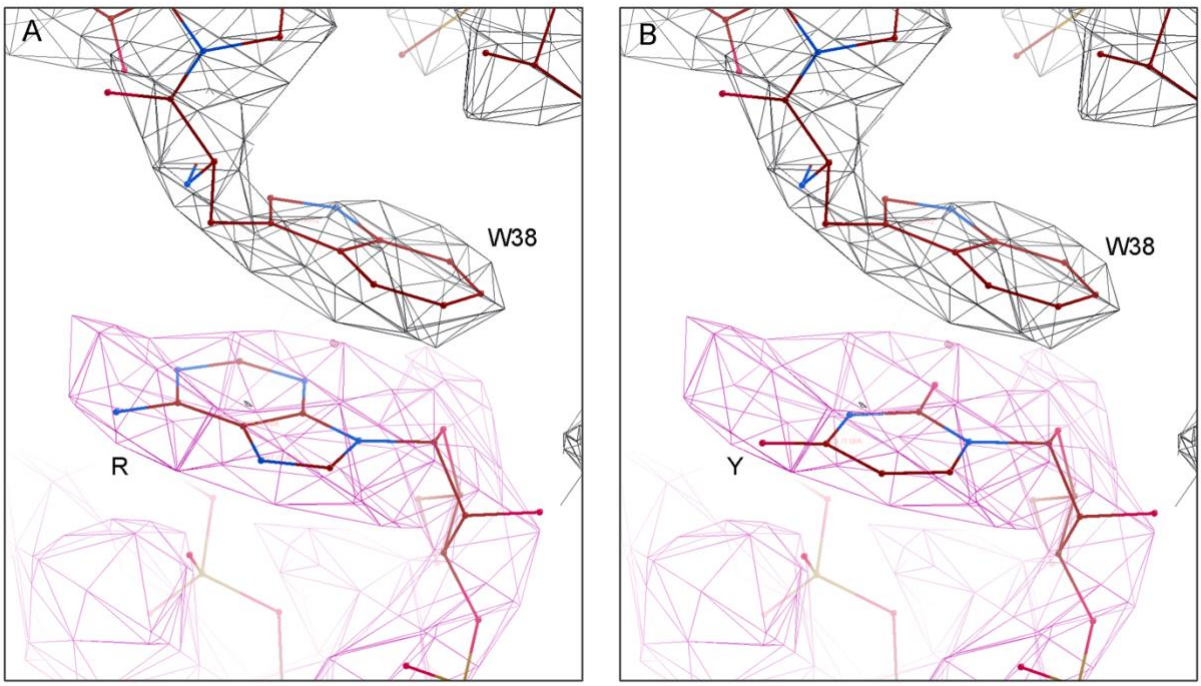

Supplementary Fig. 5. The stacking contact between the Trp38 of VP2 and the base at the end of the dsRNA segment. Comparison of (A) the fitting of a purine (R) with (B) the fitting of a pyrimidine (Y) in their cryo-EM density (pink mesh) of the RNA duplexes. Trp38 of VP2 is fitted in its cryo-EM density (black mesh).

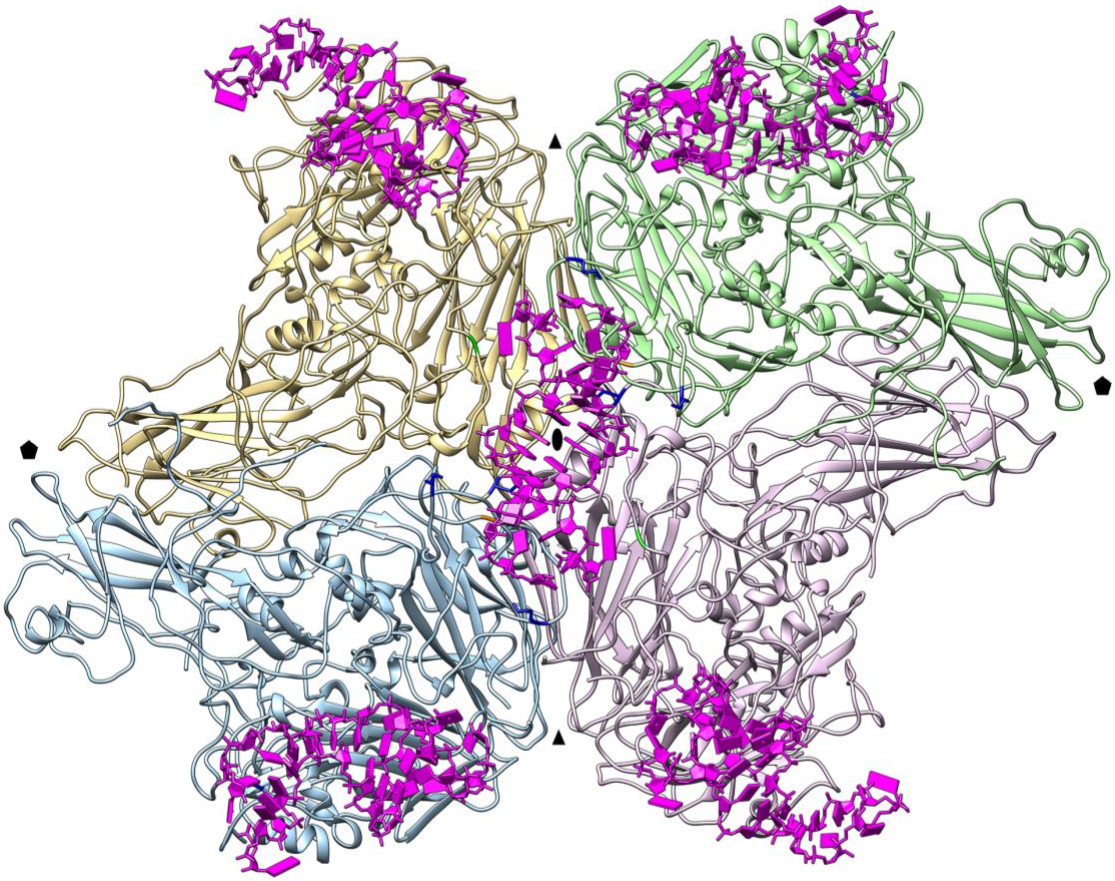

Supplementary Fig. 6. RNA duplexes in the RV-B14 virion acting as a "molecular glue" that binds capsid protomers and pentamers. A 14 bp -long dsRNA stem (pink) mediates the interaction between four 5S protomers (VP1-VP4, yellow, blue, green and violet), and each pentamer of protomers is connect with its neighbor pentamers through five dsRNA stems.

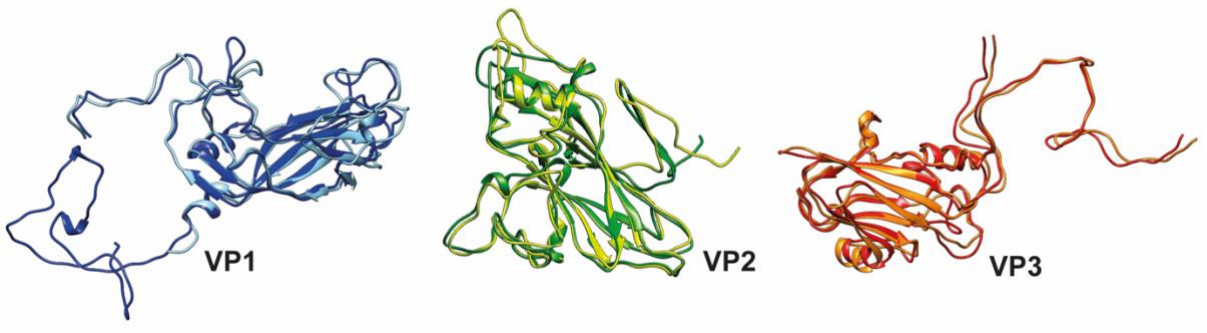

Supplementary Fig. 7. Comparison ofCP structures in the RV-B14 virion and in the empty capsid. Superimposition of VP1, VP2 and VP3 in the virion in (dark colors) and in the empty RV-B14 capsid (light colors).

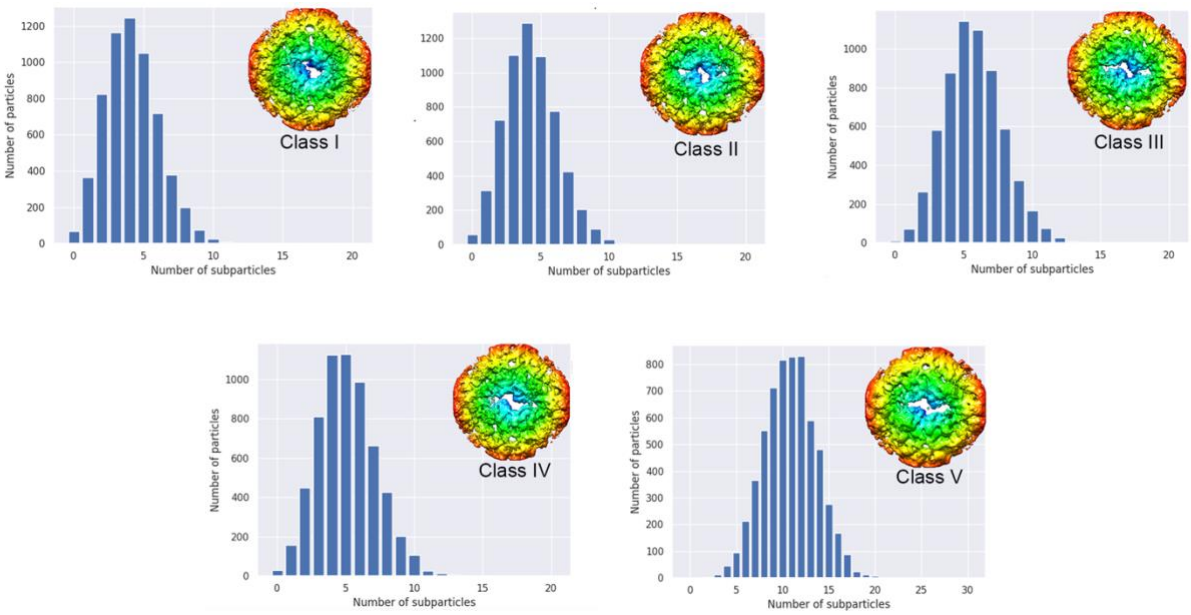

Supplementary Fig. 8. Distribution of the conformational states of the 2-fold axis pore in empty RV-B14 capsids. Histograms are shown for each of the five pore classes of pore (subparticle) classes.

Supplementary Table 1. Cryo-EM data collection and refinement statistics for RV-B14 capsids.

	Full RV-B14 EMD-17781 / PDB: 8pnf	**Empty RV-B14 EMD-17780 / PDB: 8pnb**
Data collection and processing		
Microscope	FEI Talos Arctica	FEI Talos Arctica
Voltage (kV)	200	200
Detector	Falcon III	Falcon III
Mode	Linear	Linear
Magnification	73,000x	73,000x
Electron exposure ($e^-/Å^2$)	35.1	35.1
Exposure per frame ($e^-/Å^2$)	0.54	0.54
Defocus range (μm)	-1.2 a -3.2	-1.2 a -3.2
Pixel size (Å)	1.37	1.37
Micrographs collected (no.)	4,308	4,308
Initial particles	473,724	473,724
Final particles	313,305	8,381
Symmetry imposed	I2	I2
Map resolution (Å)	2.89	3.77
FSC Threshold	0.143	0.143
Map resolution range (Å)	2.67-4.01	2.67-4.02
Refinement		
Mask correlation coefficient	0.84	0.87
Map sharpening B factor ($Å^2$)	-107	-98
Model composition (asymmetric subunit)		
Non hydrogen atoms	384,780	385,020
Protein residues	49,320	50,640
ADP (B-factors) min/max/mean	14.73/56.12/23.15	7.29/75.85/30.65
R.m.s. deviations		
Bond lengths (Å)	0.006	0.007
Bond angles (°)	0.769	0.937
Validation		
Molprobity score	1.5	1.55
Clashscore	3.8	2.92
Rotamer outliers (%)	0.38	0.59
Ramachandran plot		
Favoured (%)	95.23	92.53
Allowed (%)	4.65	7.35
Outlier (%)	0.12	0.12

Supplementary Table 2. Capsid residues involved in potential interactions with the RNA duplexes in the RV-B14 virion and their conservation in RV-B

Possible interactions with capsid-bound RNA duplexes[a]	Capsid residue	Residue conservation in RV (B species)[b]
Attractive coulombic	VP1 Lys 13	100%
	VP1 Lys 26	100%
	VP1 His 27	90%
	VP1 Lys 30	55%
	VP1 Arg 54	100%
	VP2 Lys 52	100%
	VP2 Lys 55	69%
	VP4 Lys 58	100%
van der Waals and/or H-bonds	VP1 Ile 21	45%
	VP1 Ser 22	31%
	VP1 Ser 23	97%
	VP1 Gly 24	76%
	VP1 Pro 25	55%
	VP1 Thr 28	100%
	VP2 Trp 380	100%
Repulsive coulombic	VP1 Glu 7	83%
	VP1 Glu 12	48%
	VP1 Glu 52	100%
	VP2 Glu 40	38%
	VP2 Asp 44	100%
	VP2 Asp 57	100%
	VP2 Glu 250	100%
	VP4 Asp 59	100%

[a]Cutoff distances: coulombic interactions, 10 Å (13 Å for K1013; this residue has been included because of its special position relative to the RNA duplex); hydrogen bonds (H-bonds), 3.5 Å between donor and acceptor; van der Waals interactions, 0.5 Å plus the sum of the van der Waals radii of the atoms involved. residues His27 of VP1, Lys52 and Asp44 of VP2, and Lys 58 of VP4 are also involved in van der Waals contacts and/or H-bonds with the sugar-phosphate backbone of the RNA duplexes.

[b]Percent conservation in 29 strains of the RV-B species.

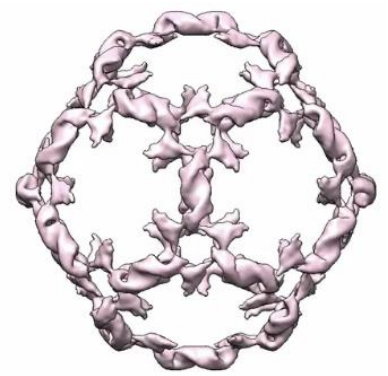

Legend to Supplementary Movie 1:
Movie depicting the internal dodecahedral cage of dsRNA filaments in RV-B14. Each dsRNA duplex contains 14 bp (blue slabs for bases).

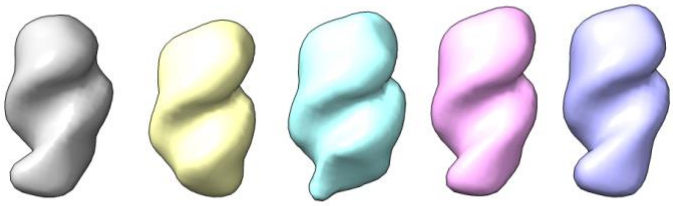

Legend to Supplementary Movie 2:
Movie depicting the five classes obtained after a focused classification on the dsRNA region at the capsid interior at the two-fold axes. Class I (grey) accounted for 8% of the total two-fold regions analyzed; class II (yellow) for another 4%; class III (cyan) for 29%; class IV (magenta) for 24%; and class V (purple) for 35%.

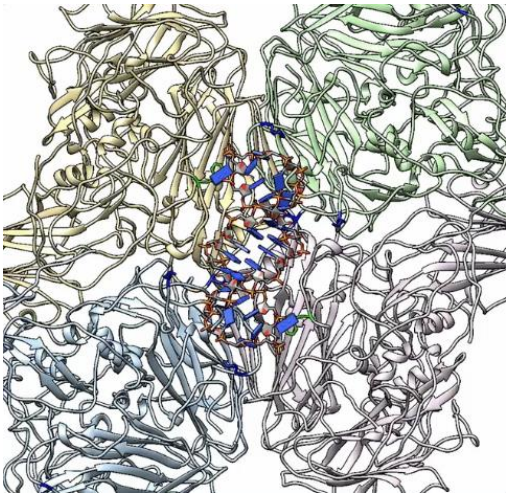

Legend to Supplementary Movie 3:
Movie depicting selected interactions between the dsRNA duplex and the capsid proteins VP1 and VP2.

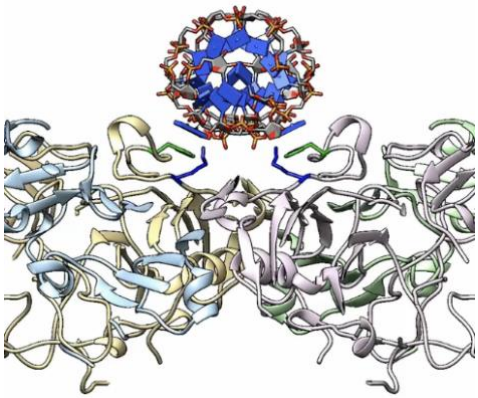

Legend to Supplementary Movie 4:
Movie depicting the transition between full and empty RV-B14 capsids, highlighting the conformational change of Trp38 (green) and Lys 52 (blue) of VP2.